Research Article

Received: 19 September 2010 Revised: 2 April 2011 Accepted: 8 May 2011 Published online in Wiley Online Library: 27 June 2011

(wileyonlinelibrary.com) DOI 10.1002/jctb.2674

Mixing and solid-liquid mass transfer characteristics in a three phase pulsed plate column with packed bed of solids in interplate spaces – a novel aerobic immobilized cell bioreactor

Vidya Shetty Kodialbail* and Govindan Srinikethan

Abstract

BACKGROUND: The pulsed plate column (PPC) with packed bed of solids in the interplate spaces finds use as a three phase aerobic bioreactor and is a potential heterogeneous catalytic reactor. Good knowledge of the extent of mixing in the liquid phase and solid-liquid mass transfer coefficient are essential for modeling, design and optimization of these columns. The present work aims at the study of liquid phase mixing and solid–liquid mass transfer characteristics in a three phase PPC.

RESULTS: Residence time distribution studies were performed. Dispersion number was found to increase with increase in liquid superficial velocities, frequency of pulsation, amplitude of pulsation and the vibrational velocities. Increase in frequency and amplitude of pulsation, and hence increase in vibrational velocity, resulted in increase of the solid–liquid mass transfer coefficient.

CONCLUSIONS: The mixing behaviour in this contactor approximated a mixed flow behaviour. The three phase PPC was found to outperform many other kinds of three phase contactors in terms of solid liquid mass transfer characteristics. Empirical correlations developed can be used for the determination of solid–liquid mass transfer coefficients for three phase PPC and hence can facilitate the design, scale-up and modeling of these columns, when used as chemical or biochemical reactors.

Keywords: dispersion number; mixing; residence time distribution; solid–liquid mass transfer coefficient; three phase pulsed plate bioreactor

NOTATION

Symbol	Description
A	pulse amplitude
A_{avg}	average surface area of benzoic acid particle
$A \times f$	vibrational velocity
a_s	surface area for solid liquid mass transfer
C_{BA}	concentration of benzoic acid in the bulk liquid at the end of the run
$C_{BA}{}^*$	solubility of benzoic acid in water
$c(t)$	tracer concentration
D	molecular diffusivity of solute in liquid
D_{ax}	axial dispersion coefficient
$\left(\frac{D_{ax}}{vL}\right)$	dispersion number
dM	weight loss of benzoic acid particle during the experimental run time
d_p	diameter of particle
$E(t)$	exit age distribution
$E(\theta)$	dimensionless exit age distribution
f	pulse frequency
k_s	solid–liquid mass transfer coefficient
L	characteristic length
N	number of tanks in series
N_s	flux of substrate from the bulk fluid to the interface
P_g/V	power input for mixing per reactor volume or the dissipated energy
Q	influent flow rate of liquid to the reactor
S_b	substrate concentration at the bulk liquid
S_s	substrate concentrations at the liquid-solid interface
t	time
$\bar{t}$	mean residence time in the reactor
T	temperature
V	volume of reactor
v	liquid superficial velocity
Sh	Sherhood number
Re_p	particle Reynolds number

* *Correspondence to: Vidya Shetty Kodialbail, Department of Chemical Engineering, National Institute of Technology Karnataka Surathkal, Srinivasnagar Post-575025, Karnataka, India. E-mail: vidyaks68@yahoo.com*

Department of Chemical Engineering, National Institute of Technology Karnataka Surathkal, Srinivasnagar Post-575025, Karnataka, India

σ^2 variance
$\sigma_\theta{}^2$ dimensionless variance
θ dimensionless time, $\frac{t}{\bar{t}}$
ρ density of liquid
μ viscosity of liquid

INTRODUCTION

A recent innovation in immobilized cell aerobic bioreactors is the pulsed plate (reciprocating plate) column with packed bed of solids in interplate spaces.[1,2] In this kind of bioreactor, the microorganisms are immobilized as a biofilm on the solids, packed in the bed. The advantages of using this kind of bioreactor over other immobilized cell systems are discussed elsewhere.[1]

Liquid phase mixing strongly influences the mass transfer rates in a gas–liquid–solid contactor. Good knowledge of the extent of mixing in the liquid phase is essential for modeling, design and optimization of these columns. Successful design and operation of a gas–liquid–solid contactor requires knowledge of the effect of various parameters that influence the axial mixing of the phases. Liquid phase mixing can be characterized experimentally through residence time distribution (RTD) studies.

Reports on axial dispersion studies in a three phase (gas-liquid-solid) pulsed plate column are very scarce and the studies to date deal only with axial dispersion in the column with a low solid content, 0–5.61% by volume.[3,4] In these studies, solid phase was regularly distributed in the axial direction, so the mixing of phases (liquid or gas and liquid) inside the column became more intensive and, consequently, the axial dispersion increased. It is essential to understand the mixing behaviour in the pulsed plate column with packed bed of solids placed in the space between the plates, so as to facilitate in the design, analysis and modeling of this column when used as a bioreactor with immobilized cells or as a heterogeneous catalytic reactor. So it was proposed to conduct RTD studies in this column to characterize the mixing behaviour and also to investigate the influence of different operating conditions on this behaviour.

The solid–liquid mass transfer coefficient is another important design parameter of gas–liquid–solid reactors for both chemical and biochemical engineering applications.[5] In three-phase biofilm reactors, if the rate of diffusion or rate of reaction within the biofilm is much faster than the liquid–solid mass transfer rate of the substrate, i.e. if the characteristic time of diffusion and reaction in the biofilm is much lower than the characteristic time of liquid–solid transfer, then the rate of mass transfer through a stagnant liquid film around the biofilm controls the whole bioprocess and the overall rate of bioprocess is said to be controlled by external mass transfer limitations. The solid–liquid mass transfer coefficient then becomes an important parameter for design, operation and modeling of three phase biofilm reactors. Accurate prediction and understanding of factors controlling the solid–liquid mass transfer are a necessary part of any design or evaluation strategy.[6]

In two phase and three phase packed beds and fluidized beds, the mass transfer coefficient is directly related to operating variables such as flow velocity, particle diameter, etc.[7,8] Solid–liquid mass transfer coefficients in a reciprocating screen stack electrochemical reactor[9] and in a tubular reactor with a single reciprocating plate agitator[10] were correlated with Reynolds numbers based on vibrational velocity ($A \times f$), where $A \times f$ is the product of amplitude and frequency of reciprocation. Similarly for rotating screen discs electrochemical reactors, Reynolds number based on rotating screen linear velocity[11] was used.

Literature on solid–liquid mass transfer in a pulsed plate column and the availability of correlations for their estimation are scarce. A correlation for solid–liquid mass transfer coefficient in a tubular reactor with single reciprocating plate agitator[10] and for packed bed columns with oscillating liquid flow[12–14] are available. But these correlations may not be applicable to the pulsed plate bioreactor, which has a number of reciprocating plates, with the fixed bed of solids present in the interplate spaces. Hence, determination of the solid–liquid mass transfer coefficient and development of correlations relating this parameter to different operating conditions in the column is essential. As benzoic acid dissolution method[15–19] is the simplest and the most popular method of obtaining the solid–liquid mass transfer coefficient, this method is used in the present study.

The present paper focuses on the study of liquid phase mixing and determination of solid–liquid mass transfer coefficient for a pulsed plate column and the effect of various operating conditions of the column on them.

MATERIAL AND METHODS

Experimental pulsed plate column

The setup comprises a cylindrical column of 5.8 cm inner diameter, consisting of a stack of five perforated plates with a plate spacing of 3 cm, mounted on a central shaft, the entire stack of plates being reciprocated by a variable drive motor. The circumference of the plate stack was covered with a nylon mesh. A schematic representation of the experimental setup is shown in Fig. 1; the experimental set up is discussed in detail elsewhere.[1] The space between the plates forming each stage in the bioreactor was filled with 1600 (approx. 40 g) glass beads of 3 mm diameter. The reactor consisted of four stages and 6400 glass beads. Glass bead packing covered approximately 60% of the height of a stage. These glass beads may serve as supports for immobilization of microorganisms when this column is used as a bioreactor or as a support to solid catalyst when used as a chemical reactor. Each plate consisted of 65 holes of 2 mm diameter drilled on a square pitch. The fractional plate free area available was 0.092. The pulsation of plate stack was generated by running the flywheel using a variable speed motor with gear reduction and frequency controller, through the slider/crank arrangement. The entire stack of plates could be pulsed at the required frequency and amplitude through this arrangement. The amplitude of pulsing motion was taken as equal to the distance between the centre of the flywheel and the centre of the hole to which the crankshaft was connected. This amplitude is half the distance traversed by a plate in the plate stack, from its maximum to minimum position, observed visually when at low speed. The frequency of pulsation was measured by counting the number of oscillations for a given period of time. The column outlet was through a port at 37 cm from the bottom of the column. The working volume of the column was 0.977 L. Tap water was pumped from the bottom of the column using a peristaltic pump. Air was supplied continuously to the column at a flowrate of 1.7–1.8 L min^{-1} and was dispersed as small bubbles into the column through four nozzles provided at the bottom portion of the guiding tube in the column. Frequency and amplitudes of pulsation were set at the required values.

Tracer experiments

Sodium chloride solution (5 mol L^{-1}) was used as a tracer. After steady liquid and airflows were attained, 5 mL of the tracer was

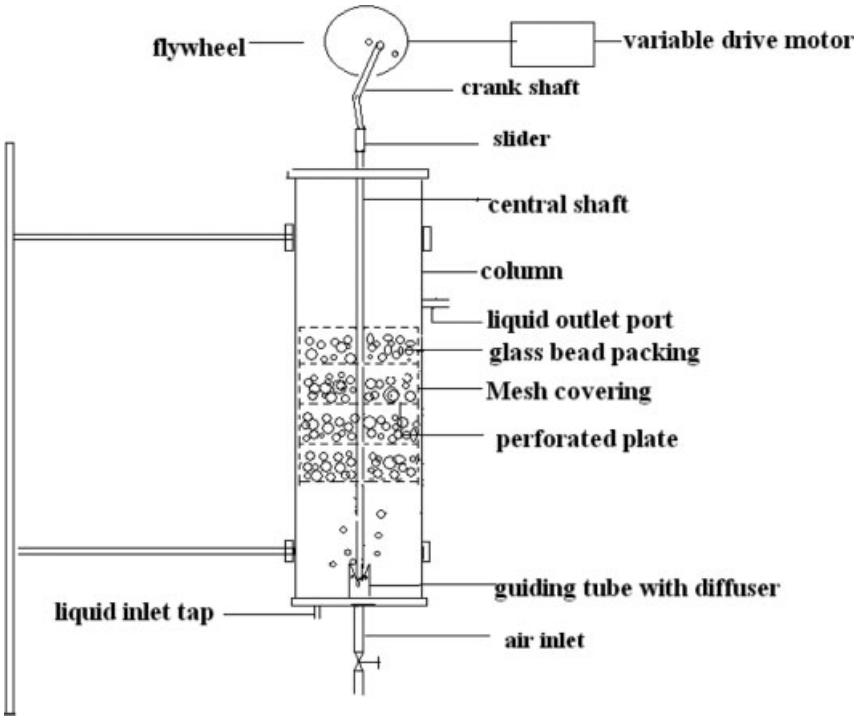

Figure 1. Experimental pulsed plate column (not to scale).

quickly injected using a syringe at a tracer injection point provided on the column wall just above the liquid feed inlet point. The tracer injection time was kept as low as possible, so as to achieve almost ideal pulse input conditions. Proper care was taken while injecting the tracer, which was injected when the plate stack was moving upward and before it started the downward motion. Water flowing out continuously from the outlet port of the column was made to flow through a constant volume flow cell. The conductivity cell was placed in the flow cell and the conductivity was measured continuously as a function of time using a Systronics digital conductivity meter (Model 304, Systronics, India) until the tracer concentration was reduced to near zero. The volume of the flow cell being less than 20 mL is only around 2% of the volume of the reactor and hence its effect on RTD of the column was considered to be negligible. Tracer experiments were conducted, at different sets of operating conditions of liquid superficial velocity (v), pulse frequency (f) and pulse amplitude (A).

Experimental method for the determination of solid–liquid (S-L) mass transfer coefficient

The flux N_s (g cm^{-2} s^{-1}) of substrate from the bulk fluid to the interface is given by:

$$N_s = k_s(S_b - S_s) \tag{1}$$

where S_b and S_s are the substrate concentrations (g cm^{-3}) at the bulk liquid and at the liquid–solid interface, respectively, and k_s is the solid–liquid mass transfer coefficient (cm.s^{-1}).

Rate of mass transfer of substrate from the bulk fluid to the interface $= k_s a_s(S_b - S_s)$ where, a_s is the surface area (cm^2) for solid–liquid mass transfer.

In the present study, the S-L mass transfer coefficients (k_s) in the pulsed plate column with four stages were determined from the rate of dissolution of individual spheres of benzoic acid into water, with air flowing at a constant rate of 1.7–1.8 L min^{-1}.

Solid benzoic acid spheres were made by using a precisely machined aluminum mold with hemispherical holes in each half of the mold. To make benzoic acid spheres, molten benzoic acid was injected into the mold, allowed to cool and then the mold was separated into two parts to remove the particles. Spheres of (4.7 ± 0.2) mm diameter were made using these molds. Final sizes were adjusted by smoothing with fine sand paper.[16,20,21]

A single active benzoic acid sphere was placed between the shaft and the mesh covering, among the glass bead packing in a particular stage. Frequency and amplitude were adjusted to required values and the reactor was filled with tap water from the top. Water and airflows were started immediately. Each run was conducted for a fixed time period (called hereafter the experimental run time or retention time for benzoic acid particle in the bed) of say 150 s. At the end of the experimental run, the water and air flow rates and the oscillations were stopped simultaneously and the water was drained immediately from the column. The time taken to start the run, after filling the column with water, was less than 25 s and for draining the water after the run, was around 10 to 15 s. The benzoic acid particle was removed from the bed and weighed. The mass transfer from the active particle was determined by measuring the weight loss of the particle over the known experimental run time (e.g. 150 s). A sample of water was collected and benzoic acid concentration in the bulk liquid during this fixed time period was determined by titration with 0.004 N NaOH solution. Surface area of the benzoic acid particle was calculated as the average value obtained by measuring the diameter before and after every run. Experiments were conducted in the same manner by keeping a benzoic acid particle in a given stage and conducting the runs for different retention times (150, 300, 450 and 600 s) of the benzoic acid particle in a stage. Separate experiments were performed by keeping the benzoic acid particles in any one stage (stages 1, 2, 3

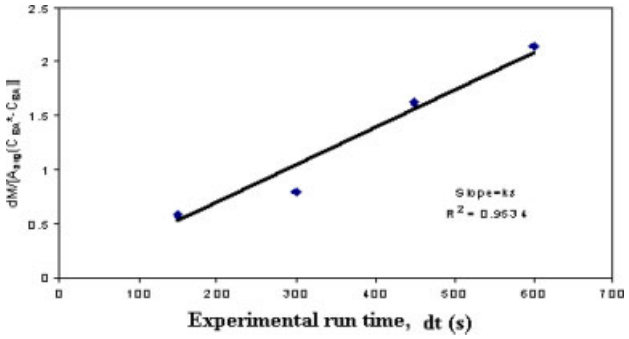

Figure 2. Representative plot for the determination of solid–liquid mass transfer coefficient for a particular stage. Conditions: $v = 12.62 \times 10^{-3}$ cm s^{-1}, $f = 0.25$ s^{-1}, $A = 3.3$ cm (for 4th stage).

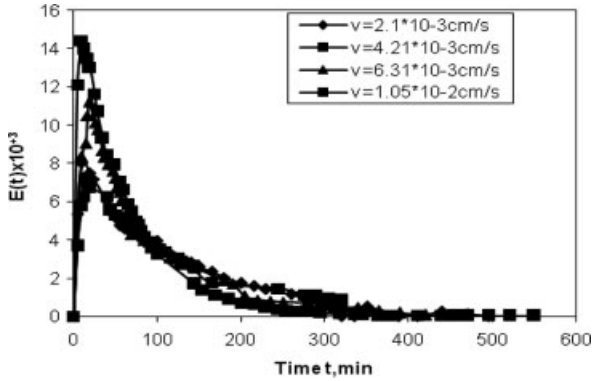

Figure 3. E curves at different liquid superficial velocities at $A = 4.7$ cm, $f = 1$ s^{-1}.

and 4) and for each stage with experimental run times of 150, 300, 450 and 600 s. For each stage and each particle retention time (experimental run time) experiment, a fresh benzoic acid particle was used. For any one experimental run, only one benzoic acid particle was used in the column.

Experiments were conducted for water flow rates of 400 mL h^{-1}, 800 mL h^{-1} and 1200 mL h^{-1} at amplitudes 3.3 cm, 4.7 cm and 6.0 cm, and for frequencies 0.25 s^{-1}, 0.50 s^{-1}, 0.75 s^{-1} and 1.0 s^{-1}. At each operating condition, benzoic acid dissolution tests were conducted for experimental run times 150 s, 300 s, 450 s, and 600s for each of the stages.

The values of mass change (weight loss) of benzoic acid particle, dM (g) during the experimental run time, dt (s), average area of the benzoic acid particle, A_{avg} (cm^2), which is the average of the values of surface area of benzoic acid particle before and after the runs, and concentration of benzoic acid in the bulk liquid, C_{BA} (g cm^{-3}) at the end of the experimental run time were obtained for each run.

Considering a completely mixed system[1] and pseudo-steady-state conditions for the bulk phase, the rate of mass transfer from solid to liquid phase can be equated to rate of change of mass of the benzoic acid particle, given by

$$dM/dt = k_s A_{avg} (C_{BA}^* - C_{BA}) \quad (2)$$

where C_{BA}^* is the solubility of benzoic acid in water at room temperature calculated as per the correlation proposed by Guedes *et al.*[20] and given by

$$C_{BA}^* = 1.44 \times 10^{-5} \exp(0.0414T) \quad (3)$$

where C_{BA}^* is in g cm^{-3} and T is the temperature in K. At 30 °C, $C_{BA}^* = 4.0386 \times 10^{-3}$ g cm^{-3}. dt is the experimental run time (e.g. 150, 300, 450 or 600 s). For a particular stage $dM/[A_{avg}(C_{BA}^* - C_{BA})]$ was calculated for each dt. A graph of $dM/[A_{avg}(C_{BA}^* - C_{BA})]$ vs. dt was plotted.[9] A representative plot is shown in Fig. 2. The slope of the best fit straight line gives the value of mass transfer coefficient for a particular stage. The mass transfer coefficient at each stage at a particular operating condition was determined using the same procedure. The average mass transfer coefficient for the column was obtained as the arithmetic mean of the mass transfer coefficients of the four stages. The particle retained its shape and the surface area of the particle decreased by less than 5% during a run. Hence the surface area could be assumed constant during the experimental run time and equal to the average of the areas before and after the run. The dissolution of a single benzoic acid particle had a negligible effect on the concentration of dissolved benzoic acid in the column. Dissolved benzoic acid concentration (C_{BA}) was in the range 5 to 16 mg L^{-1} in various runs. Since $C_{BA} << C_{BA}^*$, many researchers have used $C_{BA} = 0$ for the mass transfer coefficients determination in different types of columns. But in this study, the actual values of C_{BA} at the end of the time period of the experimental run were used for the determination of mass transfer coefficients, though negligible error would have been associated in the determination of mass transfer coefficient if $C_{BA} = 0$ was used.

To study the effect of size of benzoic acid particle used in dissolution experiments, **b**enzoic acid dissolution experiments were carried out at a water flow rate of 1200 mL h^{-1}, amplitude 4.7 cm and frequency 1 s^{-1} with benzoic acid spheres of diameter 4.8 mm and 4.1 mm.

RESULTS AND DISCUSSION

RTD studies

From the tracer experimental data, the exit age distribution $E(t)$ was calculated using

$$E(t) = \frac{c(t)}{\int_0^\infty c(t)dt} \quad (4)$$

Figures 3 to 5 show the RTD for the column under different operating conditions of superficial liquid velocities and pulse frequency and amplitudes. The RTD response clearly shows that the mixing behaviour in the column can be approximated by an ideal mixed flow behaviour. The values of the mean residence time $\bar{t}$ (s), the variance σ^2 and dimensionless variance $\sigma_\theta{}^2$ were calculated using the following equations for different operating conditions using the RTD data.

$$\bar{t} = \int_0^\infty t.E(t)dt \quad (5)$$

$$\sigma^2 = \int_0^\infty (t - \bar{t})^2.E(t)dt \quad (6)$$

$$\sigma_\theta{}^2 = \frac{\sigma^2}{\bar{t}^2} \quad (7)$$

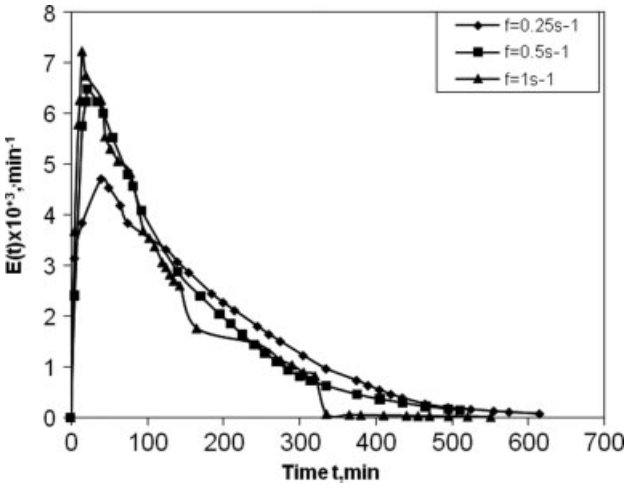

Figure 4. E curves at different pulse frequencies; at $v = 4.21 \times 10^{-3}$ cm s^{-1}; $A = 4.7$ cm.

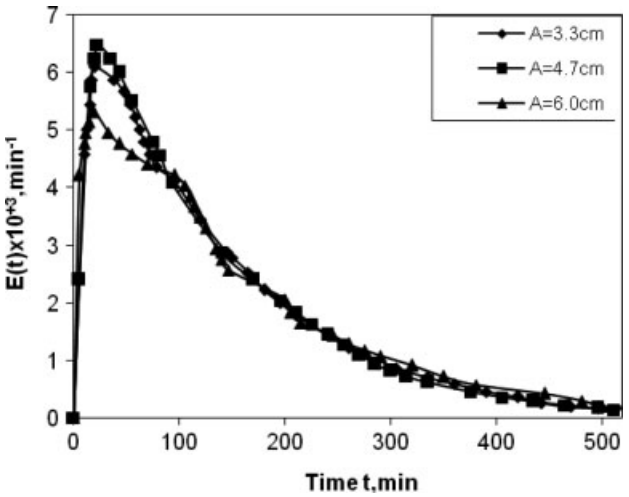

Figure 5. E curves at different pulse amplitudes at $v = 4.21 \times 10^{-3}$ cm s^{-1}; $f = 0.5$ s^{-1}.

The experimental setup used for tracer experiments in the present investigations corresponds to a closed–closed boundary with large dispersion. The method of moments a widely used and simple method, is used in the present study and the dimensionless variance was calculated from the experimental RTD data. Van der Laan[22] reported the variance for the case of closed–closed vessels as:[23–24]

$$\sigma_\theta{}^2 = \frac{\sigma^2}{\bar{t}^2} = \left(\frac{D_{ax}}{vL}\right) - 2\left(\frac{D_{ax}}{vL}\right)^2\left(1 - e^{-\frac{vL}{D_{ax}}}\right) \quad (8)$$

The dispersion number, $\frac{D_{ax}}{vL}$ is a dimensionless parameter and was calculated using Equation (8) by a trial and error method. D_{ax} (cm^2·s^{-1}) is the axial dispersion coefficient, v (cm s^{-1}) is the liquid velocity and L (cm) is the characteristic length. The number of equivalent tanks-in-series (N) were calculated using

$$N = \frac{1}{\sigma_\theta{}^2} \quad (9)$$

The variance, dispersion numbers and the number of equivalent tanks in series obtained at different operating conditions are reported in Table 1. In all cases dispersion number varies from 0.5 to 2 and the number of equivalent tanks varies from 1.17 to 1.72.

$\frac{D_{ax}}{vL} > 0.2$ and $N < 2$ signifies a large amount of dispersion[24] showing that the mixing behaviour in the column tends to a mixed flow regime. Hence the column can be approximated to be a completely mixed stirred tank. So the pulsed plate column when used as a three phase bioreactor or reactor may be considered a continuously stirred tank reactor. For substrate-inhibited bioprocesses, a bioreactor showing continuously stirred tank behaviour is favorable, unlike product-inhibited processes, where plug flow reactors are recommended. Even in cases when the substrate concentration in the influent to a completely stirred tank reactor is at inhibitory levels, the concentration of substrate in the bioreactor at steady state will be low. This may allow the organisms to be exposed to concentrations lower than inhibitory concentrations. But if a bioreactor follows plug flow behaviour, then the organisms present nearer to the entry section of the bioreactor will be exposed to inhibitory levels hence leading to lower growth and a lower rate, making inhibitory concentrations reach further sections of the reactor. This causes lower conversion in the reactor. The pulsed plate bioreactor, which approximates a mixed flow behaviour, is suitable for a substrate-inhibited processes. This aspect can be considered as one of the advantages of the pulsed plate bioreactor.

Figure 6 shows that as the superficial liquid velocity (v) increases, the dispersion number increases. Increasing the convection transport, as characterized by the liquid superficial velocity, will increase the intensity of dispersion. Similar observations were reported by several researchers based on the RTD in different kinds of contactors such as the turbulent bed contactor,[25,26] co-current down flow bubble column[27] and oscillatory-flow (pulsed sieve plate column) continuous reactor,[28] and two phase reciprocating plate columns.[29,30] According to Ni and Pereira,[31] the liquid flow rate contributes to increasing D_{ax} through the increase of mechanical energy dissipation, due to the presence of perforated plates. Prandtl's mixing length increases and Kolmogorov's length scale (designated as mixing length by Ni and Periera[31]) of eddies decreases as the flow rate increases and eddies break up. Thus the increase of superficial liquid velocity increases the turbulence and the axial dispersion. At a given air velocity, an increase in liquid velocity increases the gas hold up and axial mixing through its effect on the slip velocity between the phases.[29] As a result, the circulation and interaction of the gas and liquid phases increase inside the column and the flow becomes more agitated. This enhances the overall mixing in the column. The intimate contact between the phases increases as the gas hold-up increases, due to the stirring effect of gas on the liquid, which in turn contributes to more back mixing and turbulence in the column,[27,29] thereby further increasing the axial dispersion.

Figures 7 and 8, respectively, show the effect of frequency and amplitude of pulsation on the dispersion number. It is found that as the frequency and amplitude increases, dispersion number increases, however, the magnitude of increase of dispersion number with increase in amplitude is much less than that caused by increased frequency. The introduction of pulsation increases the mechanical energy dissipation to the system as $P \propto (A \times f)$,[3,28] due to the presence of perforated plates. According to the isotropic turbulence theory of Kolmogoroff, the axial dispersion coefficient is related to Kolmogorov's length scale ℓ (designated as mixing length by Ni and Periera[31]), and the power dissipation in a system

Table 1. Variances, dispersion numbers and number of equivalent tanks in series obtained from RTD data under different operating conditions

Sl No.	Q, mL h^{-1}	$v \times 10^{+3}$, cm s^{-1}	A, cm	f, s^{-1}	Variance, σ_θ^2	Dispersion number	Number of tanks in series
1	200	2.1	4.7	1	0.735	0.998	1.36
2	400	4.21	4.7	1	0.785	1.289	1.27
3	600	6.31	4.7	1	0.795	1.364	1.26
4	1000	10.5	4.7	1	0.854	2.027	1.17
5	400	4.21	4.7	0.25	0.581	0.526	1.72
6	400	4.21	4.7	0.5	0.667	0.736	1.5
7	400	4.21	3.3	0.5	0.660	0.716	1.51
8	400	4.21	6.0	0.5	0.697	0.836	1.44

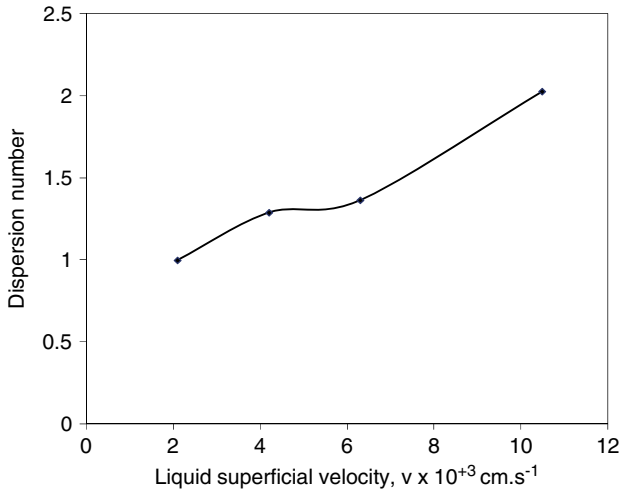

Figure 6. Effect of liquid superficial velocity on dispersion number. Conditions: $A = 4.7$ cm; $f = 1$ s^{-1}.

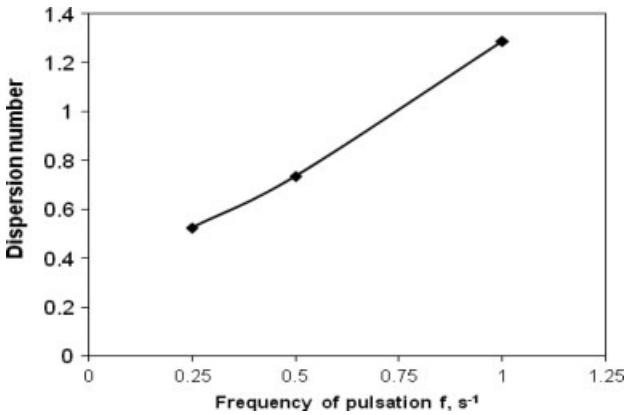

Figure 7. Effect of pulse frequency on dispersion number. Conditions: $v = 4.21 \times 10^{-3}$ cm s^{-1}; $A = 4.7$ cm.

due to mechanical agitation, P.[28,31]. Axial dispersion would increase with P and ℓ. However, the increase of P promotes turbulence and mixing of the flow, which breaks up eddies and reduces ℓ, and thus the dispersion coefficients.[31] The effect of decreased ℓ with increase of f or A is small compared with the increase of P with increase of f or A.[28] So a net increase of dispersion number can be observed with increase in amplitude or frequency. Higher amplitude of pulsation significantly increases the zone of influence

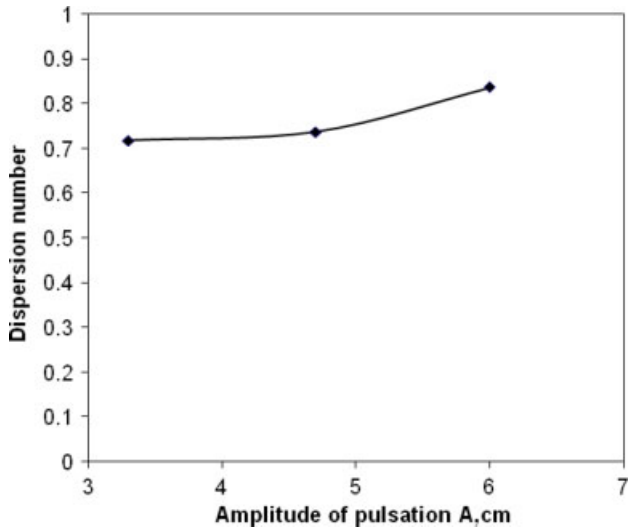

Figure 8. Effect of pulse amplitude on dispersion number. Conditions: $v = 4.21 \times 10^{-3}$ cm s^{-1}; $f = 0.5$ s^{-1}.

of the moving plates, affecting a larger zone, mixing the liquid with other portions of the liquid up and down in the column.[32] The larger pulse amplitude has, as a consequence, to drag over a longer distance the fluid contained in one elementary cell and mix it with other parts of the fluid up and down the liquid column.[33] This also contributes to an increase in dispersion number with increase in amplitude.

Figure 9 represents the effect of vibrational velocity ($A \times f$) on the dispersion number. As the vibrational velocity is increased, dispersion number is increased. Power dissipation in the system increases due to increase in mechanical agitation caused by increase in vibrational velocity; this in turn increases the dispersion number. These results are consistent with the results of previous investigators who worked on pulsed plate columns in the absence of solid phase, where continuous phase axial mixing was found to increase with increase in ($A \times f$) or with the increase in the power input, which is proportional to $[(A \times f)^3]$.[29,30,34–39] The application of oscillatory motion can also increase gas hold up through its ability to retard the rise velocity of bubbles and increase its residence time in the column.[40] Furthermore, the increase in energy dissipation rate results in the formation of smaller bubble sizes with smaller rise velocity and consequently higher gas hold up and interfacial areas, which would then increase the axial mixing due to turbulence, circulation and phase entrainment induced by the rising bubbles.[29]

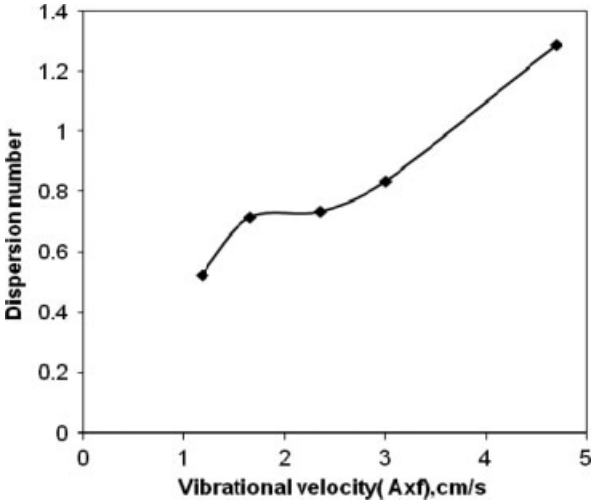

Figure 9. Effect of vibrational velocity on dispersion number. Conditions: $v = 4.21 \times 10^{-3}$ cm s^{-1}.

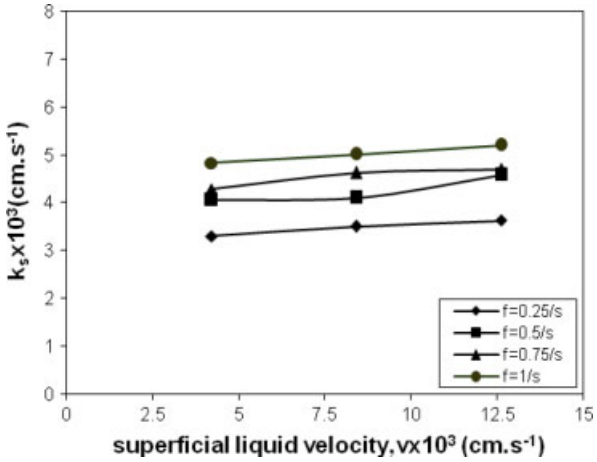

Figure 10. Effect of superficial liquid velocities on S-L mass transfer coefficients at different pulse frequencies and at $A = 3.3$ cm.

Table 2. Effect of the size of benzoic acid sphere on mass transfer coefficient	
Diameter of benzoic acid sphere (mm)	$k_s \times 10^3$ (cm/s)
4.8	7.235
4.1	7.182

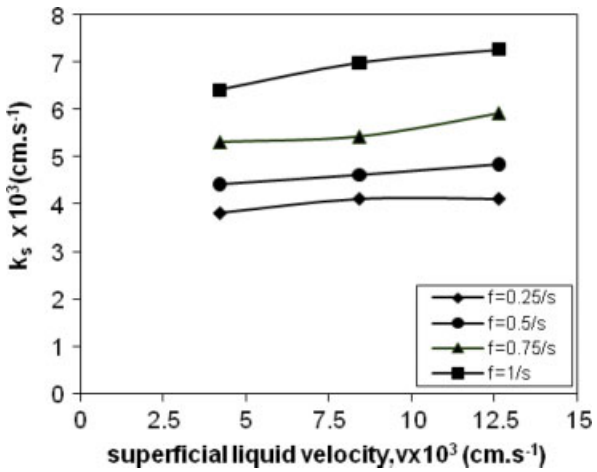

Figure 11. Effect of superficial liquid velocities on S-L mass transfer coefficient at different pulse frequencies and at $A = 4.7$ cm.

Solid–liquid mass transfer coefficients

Effect of the size of benzoic acid sphere on S-L mass transfer coefficient

S-L mass transfer coefficients were determined at water flow rate (Q) of 1200 mL h^{-1} (superficial liquid velocity, $v = 12.62 \times 10^{-3}$ cm s^{-1}), $A = 4.7$ cm and $f = 1$ s^{-1} with two different sized benzoic acid spheres. The mass transfer coefficients calculated are presented in Table 2, which shows that there is a negligible difference (around 0.7%) in the mass transfer coefficients with change in size of the particles. So spherical particles with a diameter range 4.7 ± 0.2 mm were used for further experimentation, as obtained after molding without any adjustments of dimensions. The independence of k_s with particle diameter was reported by Arters and Fan[17] for particles with diameter in the range 1.6 to 4.5 mm in the gas–liquid–solid fluidized bed at gas velocities less than or equal to 6.6 cm s^{-1}. Jadhav and Pangarkar[41] reported the independence of k_s for particle size above 2.23 mm in a three phase sparged reactor. It should also be noted that Jianping *et al*.[6] observed that the S-L mass transfer coefficient is quite independent of the solid particle diameters in the range 3 to10 mm. So in the present work, though the solid–liquid mass transfer coefficient was determined using a benzoic acid sphere of diameter 4.7 ± 0.2 mm, these coefficients would be applicable to a column with glass spheres of 3 mm diameter.

Effect of operating conditions on S-L mass transfer coefficient

Effect of superficial liquid velocity

The effect of superficial liquid velocity on the liquid solid mass transfer coefficient at different frequencies (0.25, 0.5, 0.75 and 1 s^{-1}) and at amplitudes of 3.3, 4.7 and 6.0 cm are presented in Figs 10 to 12. Different superficial liquid velocities used were 4.21×10^{-3}, 8.41×10^{-3}, 12.62×10^{-3} cm s^{-1}, corresponding to liquid flow rates of 400, 800 and 1200 mL h^{-1}. Marginal or no significant increase in mass transfer coefficient is observed with increase in superficial liquid velocity. Increase in S-L mass transfer coefficient with increase in liquid velocity was expected, as higher liquid velocity promotes a higher degree of turbulence of liquid and makes the mass transfer liquid film around the particle, thinner. But the turbulence created by increasing the liquid velocity is negligible compared with the turbulence created by reciprocation of the plates.[42–44] So there was only a marginal or no significant increase in mass transfer coefficient with liquid velocity. Similar observations were made by other researchers in different columns such as the packed bed column,[45] fluidized bed column,[17–19,46] three-phase reversed flow jet loop reactor[6] and three phase catalytic upflow reactor.[47]

The range of values of liquid solid mass transfer coefficients obtained at frequencies of 0.25, 0.5, 0.75 and 1 s^{-1}, shows that the contribution of turbulence intensity to the value of liquid solid mass transfer coefficient by plate pulsation is much more than that due to liquid flow.

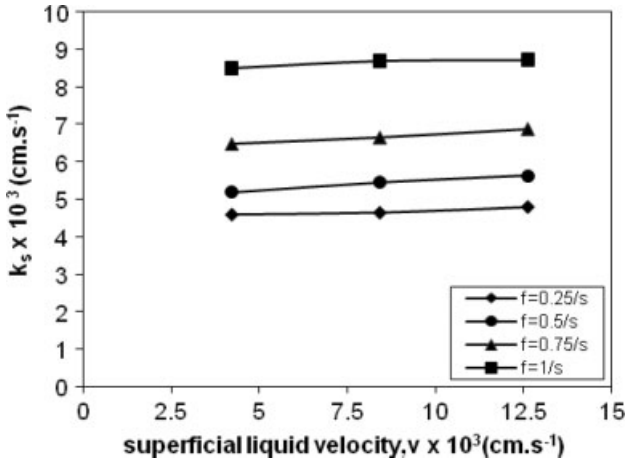

Figure 12. Effect of superficial liquid velocities on S-L mass transfer coefficients at different pulse frequencies and at $A = 6.0$ cm.

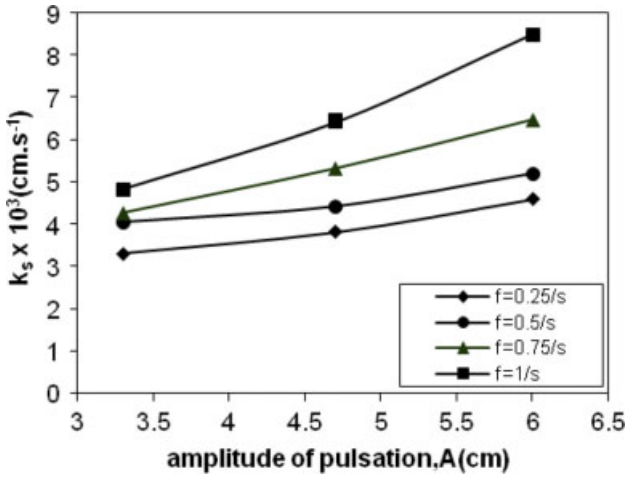

Figure 13. Effect of pulse amplitude on S-L mass transfer coefficients at different pulse frequencies and at $v = 4.21 \times 10^{-3}$ cm s^{-1}.

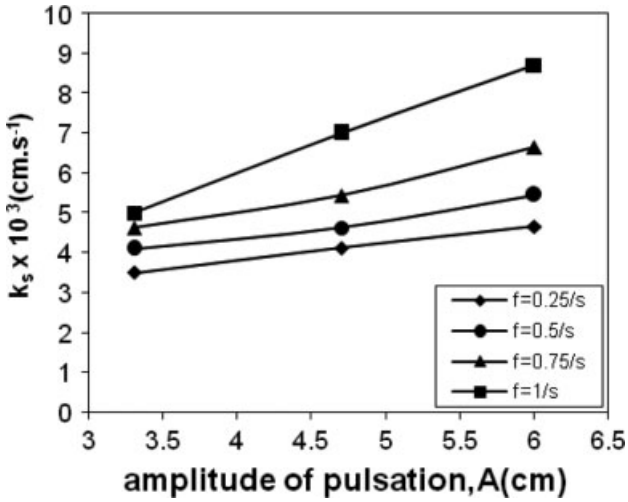

Figure 14. Effect of pulse amplitude on S-L mass transfer coefficient at different pulse frequencies and at $v = 8.41 \times 10^{-3}$ cm s^{-1}.

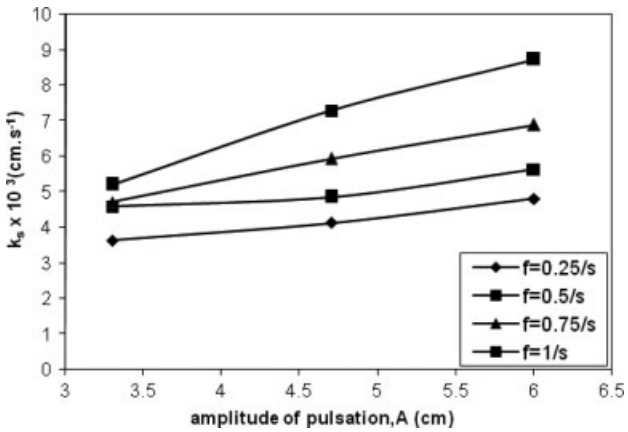

Figure 15. Effect of pulse amplitude on S-L mass transfer coefficient at different pulse frequencies and at $v = 12.6 \times 10^{-3}$ cm s^{-1}.

Effect of frequency and amplitude of pulsation

The effect of frequency and amplitude of pulsation on the liquid solid mass transfer coefficient at different superficial liquid velocities ($v = 4.21 \times 10^{-3}$, 8.41×10^{-3}, 12.62×10^{-3} cm s^{-1}) are presented in Figs 13 to 15. The solid–liquid mass transfer coefficient was found to increase with increase in frequency and amplitude of pulsation. Frequency of pulsation periodically renews the surface available for mass transfer and also thins down the liquid film thickness around the solid particle and hence decreases the mass transfer resistance. This results in an increase of mass transfer coefficient with increasing frequency. The increase in solid–liquid mass transfer coefficient with frequency was found to be greater at larger amplitudes. Changes in oscillation amplitude affected the mass transfer coefficient more than changes in oscillation frequency, since the amplitude of oscillation controls the length of eddy generated along the column.[48] Fig. 16 shows that the S-L mass transfer coefficients increase with increase in vibrational velocity ($A \times f$). As the frequency or amplitude of pulsation increases, vibrational velocity increases. The periodically reversing fluid motion with higher amplitudes and frequencies interacts with the plates, forming vortices and hence turbulence. The power dissipation in a system due to mechanical agitation is proportional to $[(A \times f)^3]$.[28] The increase in power dissipation promotes greater turbulence and mixing in the liquid phase[29] resulting in thinner liquid film around the solid particle. So the resistance offered to mass transfer decreases and hence the mass transfer coefficient increases.

Empirical correlation for the determination of solid–liquid mass transfer coefficient

Using the experimental values of mass transfer coefficients determined in this study, dimensional and dimensionless empirical correlations were developed by nonlinear regression using LABFIT software. Dimensional correlation relates k_S with liquid superficial velocity, frequency and amplitude of pulsation at a fixed airflow rate of 1.7 to 1.8 L min^{-1} as below:

$$k_s = 3.23 \times 10^{-3} A^{0.6838} f^{0.4057} v^{0.06818} \quad (10)$$

with k_s in cm s^{-1}, A in cm, f in s^{-1}, and v in cm s^{-1}.

The correlation is valid within the following range : $3.3 \leq A \leq 6.0$; $0.25 \leq f \leq 1.0$; $4.21 \times 10^{-3} \leq v \leq 12.62 \times 10^{-3}$. Correlation coefficient was found to be 0.959. A plot of predicted values of k_s vs. experimental k_s in Fig. 17, shows the goodness of fit of the correlation.

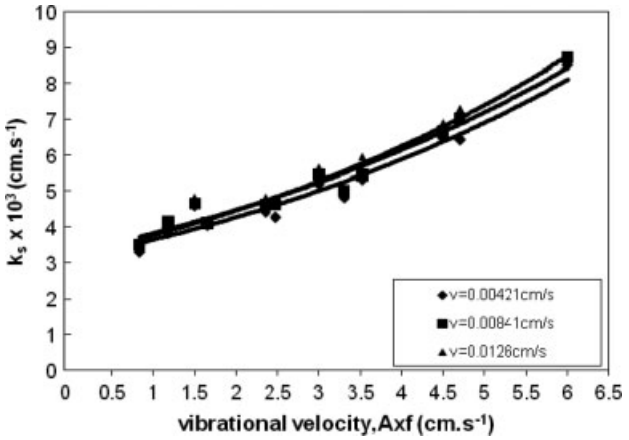

Figure 16. Effect of vibrational velocity on S-L-mass transfer coefficient at different superficial liquid velocities.

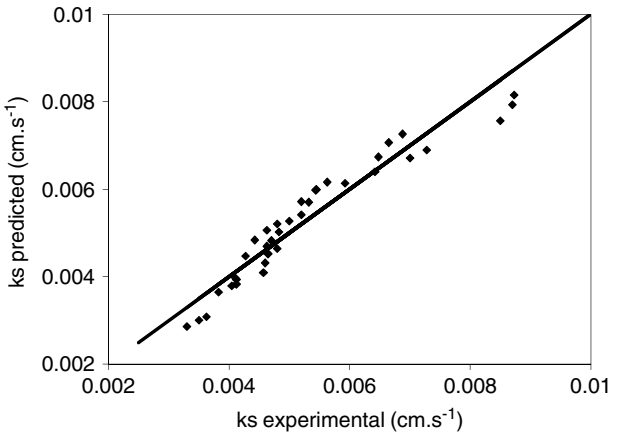

Figure 17. Correlation between predicted value of k_s and experimental k_s.

Dimensionless correlation relates Sherwood number (*Sh*) with the ratio of vibrational velocity to flow velocity ($\frac{A \times f}{v}$) and the particle Reynolds number (Re_p) based on the diameter of inert particles (glass bead), at a fixed airflow rate of 1.7 to 1.8 L min^{-1} as below:

$$Sh = 16.14 \left(\frac{A \times f}{v}\right)^{0.4668} (Re_p)^{0.5371} \quad (11)$$

where

$$Sh = \frac{k_s d_p}{D}$$

$$Re_p = \frac{\rho d_p v}{\mu}$$

Here, D is the molecular diffusivity of solute in liquid, ρ is the density of liquid, d_p is the diameter of inert particles in the bed (glass bead diameter), and μ is the viscosity of liquid. The correlation is valid within in the following range:

$$65 \leq \left(\frac{A \times f}{v}\right) \leq 1425$$

$$0.158 \leq Re_p \leq 0.473$$

The correlation coefficient was found to be 0.933. A plot of predicted values of *Sh* vs. experimental *Sh* in Fig. 18 shows the goodness of fit of the correlation.

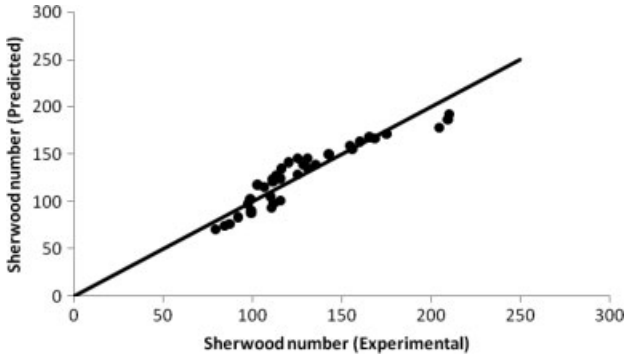

Figure 18. Correlation between predicted value of *Sh* and experimental *Sh*.

Dimensional correlation was found to fit the experimental data better than the nondimensional correlation.

These correlations can be used for the determination of S-L mass transfer coefficient under different operating conditions in the three phase pulsed plate column.

Comparison with other types of contactor

The mass transfer coefficients in a pulsed plate column with a packed bed of particles of diameter 3 mm, ranged from 3×10^{-3} cm s^{-1} to 9×10^{-3} cm s^{-1} at superficial liquid velocities of 4.21×10^{-3} to 12.62×10^{-3} cm s^{-1} and at a superficial gas velocity of 1.45 cm s^{-1}. These values are compared with those in other kinds of three phase contactors.

In a three phase sparged reactors with stagnant liquid phase and continuous gas phase with superficial gas velocity 9 to 35 cm s^{-1}, with particle sizes ranging from 0.5 to 4 mm, k_s values ranged from 4×10^{-3} to 6×10^{-3} cm s^{-1}.[41] In a three phase fluidized bed column with liquid superficial velocities 3 to 7 cm s^{-1} and gas velocity 10 cm s^{-1} the mass transfer coefficient was around 8×10^{-3} cm s^{-1}.[19] Though these values of k_s are of a similar order of magnitude to those of the pulsed plate column, the gas velocities involved in these cases are around 6–24 times more than those used in the pulsed plate column.

In a three phase draft tube fluidized bed column at liquid superficial velocities of 5.6×10^{-3} cm s^{-1} to 9×10^{-3} cm s^{-1} and air superficial velocities of 1.68 to 3.38 cm s^{-1} the mass transfer coefficients were reported to be 5×10^{-5} to 2×10^{-4} cm s^{-1}.[46] The pulsed plate column outperforms the draft tube fluidized bed column by one to two orders of magnitude in terms of solid liquid mass transfer, even at lower air superficial velocity than those used in a draft tube fluidized bed column.

In a multiphase external loop airlift reactor, the solid–liquid mass transfer coefficient was found to be constant at 1.8×10^{-3} cm s^{-1}, as the superficial air velocity was increased from 0.5 to 4.2 cm s^{-1}.[49] Though the mass transfer coefficient was of the same order of magnitude as in the pulsed plate column, the value is less than those of the pulsed plate column under similar air velocities.

In a three phase reversed flow jet loop column, the solid liquid mass transfer coefficient obtained was 8×10^{-3} cm s^{-1} at a liquid velocity of 17.6 cm s^{-1} and air velocity of 2.46 cm s^{-1}. The liquid velocity used here was around three orders of magnitude higher, and the air velocity used was marginally higher than those used in the present study. With these higher flow velocities, the order of magnitude of the value of k_s in a three phase reversed flow jet loop column is similar to those obtained for the pulsed plate column in the present study.

These comparisons show that the three phase pulsed plate column with a packed bed of solids, outperforms many other kinds of three phase contactor in terms of solid–liquid mass transfer characteristics.

CONCLUSIONS

It can be concluded from RTD studies, that the mixing behaviour in the three phase pulsed plate column with a packed bed of solids in the interplate spaces, approximates to a mixed flow behaviour and hence is suitable for substrate-inhibited bioprocesses. The dispersion number was found to increase with increase in liquid superficial velocities, pulse frequency, pulse amplitude, and vibrational velocities.

The solid–liquid mass transfer coefficient was found to increase with increase in frequency and amplitude of pulsation and hence with increase in vibrational velocity. There was only a marginal or no significant increase in mass transfer coefficient with liquid superficial velocity. A dimensional empirical correlation was developed relating k_S with liquid superficial velocity, pulse frequency and amplitude and a dimensionless correlation was developed relating Sherwood number with $\frac{A \times f}{v}$ and particle Reynolds number, at a fixed airflow rate of 1.7 to 1.8 L min^{-1}. These correlations can be used for the determination of S-L mass transfer coefficient for the three phase pulsed plate column under different operating conditions. The three phase pulsed plate column with packed bed of solids was found to outperform many other kinds of three phase contactor in terms of solid–liquid mass transfer characteristics.

REFERENCES

1 Shetty KV, Kalifathulla I and Srinikethan G, Performance of pulsed plate bioreactor for biodegradation of phenol. *J Hazard Mater* **140**:346–352 (2007).
2 Shetty KV, Ramanjaneyulu R and Srinikethan G, Biological phenol removal using immobilized cells in a pulsed plate bioreactor: effect of dilution rate and influent phenol concentration. *J Hazard Mater* **149**:452–459 (2007).
3 Nikolic LB, Nikolic VD, Veljkovic VB, Lazic ML and Skala DU, Axial dispersion of the liquid phase in a three-phase Karr reciprocating plate column. *J Serb Chem Soc* **69**:581–599 (2004).
4 Nikolic LB, Veljkovic VB and Skala DU, Analysis of liquid flow in a Karr reciprocating plate column. *Chem Ind* **55**:249–254 (2001).
5 Nicolella C, van Loosdrecht MCM and Heijnen JJ, Identification of mass transfer parameters in three-phase biofilm reactors. *Chem Eng Sci* **54**:314–331 (1999).
6 Jianping W, Lin H, Yong Z, Chao L and Yunlin C, Solid–liquid mass transfer in a gas–liquid–solid three-phase reversed flow jet loop reactor. *Chem Eng J* **78**:231–235 (2000).
7 Laguerie C and Angelino H, A few comments on particle to liquid mass transfer in fluidized bed. *Chem Eng Sci* **30**:1525–1526 (1975).
8 Evans GC and Gerald GF, Mass transfer from benzoic acid granules to water in fixed and fluidized beds at low Reynolds numbers. *Chem Eng Prog* **49**:135–140 (1953).
9 Zaki MM, Nirdosh I and Sedahmed GH, Mass transfer characteristics of reciprocating screen stack electrochemical reactor in relation to heavy metal removal from dilute solutions. *Chem Eng J* **126**:67–77 (2007).
10 Masiuk S, Dissolution of solid body in a tubular reactor with reciprocating plate agitator- Short communication. *Chem Eng J* **83**:139–144 (2001).
11 Sedahmed GH, Al-Abd MZ, Al-Taweel YA and Darwish MA, Liquid-solid mass transfer behaviour of rotating screen discs- Short communication. *Chem Eng J* **76**:247–252 (2000).
12 Zaki MM, Nirdosh I, Baird MHI and Sedahmed GH, Effect of superimposed pulsating flow on liquid-solid mass transfer in fixed beds. *Can J Chem Eng* **83**:593–598 (2005).
13 Condoret S, Riba JP and Angelino H, Mass transfer in a particle bed with oscillating flow. *Chem Eng Sci* **44**:2107–2111 (1989).
14 Wu R, McCready MJ and Varma A, Influence of mass transfer coefficient fluctuation frequency on performance of three-phase packed-bed reactors. *Chem Eng Sci* **50**:3333–3344 (1995).
15 Tang WT, Wisecarver K and Fan LS, Dynamics of a draft tube gas-liquid-solid fluidized bed bioreactor for phenol degradation. *Chem Eng Sci* **42**:2123–2134 (1987).
16 Guo G and Thompson K, Experimental analysis of local mass transfer in packed beds. *Chem Eng Sci* **56**:121–132 (2001).
17 Arters DC and Fan LS, Solid–liquid mass transfer in a gas-liquid-solid fluidized bed. *Chem Eng Sci* **41**:107–115 (1986).
18 Arters DC and Fan LS, Experimental methods and correlation of solid–liquid mass transfer in fluidized beds. *Chem Eng Sci* **45**:965–975 (1990).
19 Prakash A and Briens CL and Bergougnou MA, Mass transfer between solid particles and liquid in a three phase fluidized bed. *Can J Chem Eng* **65**:228–236 (1987).
20 Guedes de Carvalho JRF, Delgado JMPQ and Alves MA, Mass transfer between flowing fluid and sphere buried in packed bed of inerts. *AIChE J* **50**:65–74 (2004).
21 Guedes de Carvalho JRF and Delgado JMPQ, Mass transfer from a large sphere buried in a packed bed along which liquid flows. *Chem Eng Sci* **54**:1121–1129 (1999).
22 Van der Laan ETL, Notes on the diffusion type model for the longitudinal mixing in flow. *Chem Eng Sci* **7**:187–191 (1958).
23 Zarook SM, Sheik AA and Azam SM, Axial dispersion in biofilters. *Biochem Eng J* **1**:77–84 (1998).
24 Levenspiel O, *Chemical Reaction Engineering*, 2nd edn. John Wiley & Son Inc., New York (1972).
25 Bruce AER, Vinay WA, Sai PST and Krishnaiah K, Estimation of liquid phase mixing due to solids in a turbulent bed contactor. *Chem Eng Sci* **61**:3403–3408 (2006).
26 Bruce AER, Sai PST and Krishnaiah K, Characterization of liquid phase mixing in turbulent bed contactor through RTD studies. *Chem Eng J* **104**:19–26 (2004).
27 Majumder SK, Kundu G and Mukherjee D, Mixing mechanism in a modified co-current downflow bubble column. *Chem Eng J* **112**:45–55 (2005).
28 Mauri Palma and Reinaldo Giudici, Analysis of axial dispersion in an oscillatory-flow continuous reactor. *Chem Eng J* **94**:189–198 (2003).
29 Gomma HG and Al Taweel AM, Axial mixing in a novel pilot scale gas liquid reciprocating plate column. *Chem Eng Process* **44**:1285–1295 (2005).
30 Parthasarathy P, Srinikethan G, Srinivas NS and Varma YBG, Axial mixing of continuous phase in reciprocating plate columns. *Chem Eng Sci* **39**:987–995 (1984).
31 Ni X and Pereira NE, Parameters affecting fluid dispersion in a continuous oscillatory baffled tube. *AIChE J* **46**:37–45 (2000).
32 Lounes M and Thibault J, Axial mixing in a reciprocating plate column. *Can J Chem Eng* **74**:187–194 (1996).
33 Lounes M and Thibault J, Mass transfer in a reciprocating plate bioreactor. *Chem Eng Commun* **127**:169–189 (1994).
34 Baird MHI and Rama Rao NV, Axial mixing in a 15 cm diameter reciprocating plate bubble column. *Can J Chem Eng* **76**:370–378 (1998).
35 Baird MHI and Rama Rao NV, Characteristics of a countercurrent reciprocating plate bubble column.II. Axial mixing and mass transfer. *Can J Chem Eng* **66**:222–230 (1988).
36 Baird MHI, Rama Rao NV and Vijayan S, Axial mixing and mass transfer in a vibrating perforated plate extraction column. *Can J Chem Eng* **70**:69–76 (1992).
37 Karr AE, Ramanujam S, Lo TC and Baird MHI, Axial mixing and scale up of reciprocating plate columns. *Can J Chem Eng* **65**:373–381 (1987).
38 Srinikethan G, Prabhakar A and Varma YBG, Axial dispersion in plate pulsed columns. *Bioprocess Eng* **2**:161–168 (1987).
39 Hafez MM, Baird MHI and Nirdosh I, Flooding and axial dispersion in reciprocating plate extraction columns. *Can J Chem Eng* **57**:150–158 (1979).
40 Rama Rao NV and Baird MHI, Axial mixing and gas hold up with reciprocating doughnut plates. *Can J Chem Eng* **78**:261–264 (2000).
41 Jadhav SV and Pangarkar VG, Particle–liquid mass transfer in three phase sparged reactor. *Can J Chem Eng* **66**:572–578 (1988).
42 Harikrishnan TL, Prabhakar A and Varma YBG, Apparent and true longitudinal concentration profiles in reciprocating plate column. *Bioprocess Eng* **9**:23–30 (1993).

43 Shen ZJ, Rama Rao NV and Baird MHI, Mass transfer in a reciprocating plate extraction column. Effects of mass transfer direction and plate material. *Can J Chem Eng* **63**:29–36 (1985).
44 Tojo K, Miyanami K and Yano T, Liquid-liquid extraction in a multistage vibrating disk column. *J Chem Eng Japan* **8**:122–126 (1975).
45 Boskovic-Vragolovic N, Brzic D and Grbavcic Z, Mass transfer between a fluid and an immersed object in liquid–solid packed and fluidized beds. *J Serb Chem Soc* **70**:1373–1379 (2005).
46 Venu Vinod A and Reddy GV, Mass transfer correlation for phenol biodegradation in a fluidized bed bioreactor. *J Hazard Mater* **B136**:727–734 (2006).
47 Stuber F, Wilhelm AM and Delmas H, Modeling of three phase catalytic upflow reactor: a significant chemical determination of liquid-solid and gas-liquid mass transfer coefficients. *Chem Eng Sci* **51**:2161–2167 (1996).
48 Ni X and Gao S, Scale-up correlation for mass transfer coefficients in pulsed baffled reactors. *Chem Eng J* **63**:157–166 (1996).
49 Mao HH, Chisti Y and Moo-Young M, Multiphase hydrodynamics and solid–liquid mass transport in an external-loop airlift reactor – a comparative study. *Chem Eng Commun* **113**:1–13 (1992).

